COMMUNICATION

ChemComm
www.rsc.org/chemcomm

High surface area graphitized carbon with uniform mesopores synthesised by a colloidal imprinting method†

Zuojiang Li,[a] Mietek Jaroniec,*[a] Young-Jae Lee[b] and Ljubisa R. Radovic[b]

[a] *Department of Chemistry, Kent State University, Kent, Ohio 44242, USA. E-mail: jaroniec@kent.edu*

[b] *Department of Energy and Geo-Environmental Engineering, The Pennsylvania State University, University Park, PA 16802, USA. E-mail: lrr3@psu.edu*

Received (in Purdue, IN, USA) 17th January 2002, Accepted 9th April 2002
First published as an Advance Article on the web 22nd May 2002

Heat treatment of mesoporous carbons obtained by colloidal imprinting of mesophase pitch particles was used to prepare graphitized carbons with uniform mesopores and high surface area.

There is a great interest in the synthesis of mesoporous carbons because of their applications in adsorption and separation of large organic compounds, double layer capacitors and rechargeable batteries.[1–3] Although there are many papers about adsorption phenomena on graphitized carbons, the literature related to the control of their porosity is rare because these carbons are primarily used in industry as nonporous materials due to their high electrical and thermal conductivity and chemical stability. Graphitized carbon blacks developed for gas chromatography and industrial applications, which are agglomerates of primary nanoparticles, exhibit rather poor mechanical strength.[4] Knox and Kaur reported the synthesis of graphitized porous carbons for liquid chromatography by impregnation of porous silica with phenolic resin and subsequent carbonization.[5] Klett *et al*. reported the synthesis of graphitized carbon foams of high thermal conductivity, which are essentially macroporous materials.[6] Indeed, the control of mesoporosity in graphitized carbons is difficult because graphitization often leads to significant deterioration of porous structure, especially in the range of micropores and mesopores. Recently, great progress has been made in the synthesis of carbons with ordered mesopores by using highly ordered silicas such as MCM-48 and SBA-15 as templates.[7–9] However, there are some limitations in this procedure. For example, carbons synthesized by using MCM-48 of different pore sizes as templates[8] exhibit the same pore width because their pore size is determined by the wall thickness of ordered silica templates, which is usually about 1–3 nm. Colloidal crystals have also been used as templates to prepare highly ordered carbons.[10–13] Nevertheless, this approach seems to be appropriate for synthesis of ordered macroporous carbons. In addition, these carbons are often obtained by impregnating colloidal crystals with organic precursors such as sucrose and therefore possess an appreciable number of complementary micropores.

The recently reported colloidal imprinting method[14] was shown to be successful for synthesis of mesoporous carbons with uniform spherical pores. This simple method allowed an effective control of the mesoporous structure of the resulting carbons by selecting proper silica colloids and adjusting the extent of imprinting. In addition, the complementary microporosity, which results from the nature of carbon precursors used such as sucrose or poly(furfuryl alcohol), was significantly reduced by using a mesophase pitch as the precursor.

Here we demonstrate that the colloidal imprinting of mesophase pitch particles allows one to synthesise graphitized carbons with uniform spherical mesopores and high surface area. Also, this method allows one to tailor the resulting pore size in the range of mesopores and macropores by simply selecting the size of siliceous colloids used as templates. In addition, the colloidal imprinting is suitable for synthesis of the volume- and surface-imprinted mesoporous carbons.

The preparation procedure of mesoporous graphitized carbons includes colloidal imprinting, carbonization, template dissolution and graphitization. The first three steps shown in Scheme 1 were carried out as reported in ref. 14. The colloid-imprinted carbon denoted in ref. 14 as CIC-24C was graphitized. The graphitization was carried out under protection of argon using a heating rate of 10 °C min^{-1} until a temperature of 2400 °C was reached, and it was continued for 60 min at 2400 °C followed by cooling the sample to room temperature under an argon atmosphere. The resulting graphitized sample is denoted CIC-24C-G.

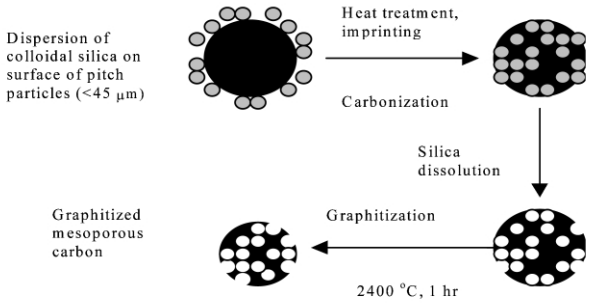

Scheme 1 Synthesis of graphitized carbon with uniform spherical mesopores.

Nitrogen adsorption (−196 °C) was employed to study the pore structure of carbonized and graphitized samples. Fig. 1 shows isotherms of the graphitized colloid-imprinted carbon and the corresponding sample before graphitization but after carbonization at 900 °C. For comparison, the isotherm of the commercial graphitized carbon black Carbopack X is also included. All isotherms exhibit the type H1 hysteresis loop at higher relative pressure[15] indicating capillary condensation in

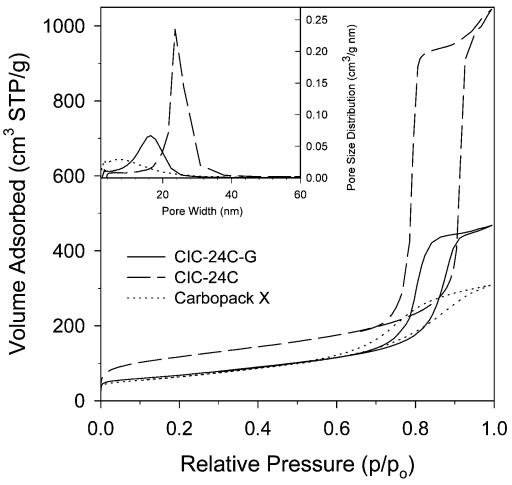

Fig. 1 Nitrogen adsorption isotherms at –196 °C and the corresponding pore size distributions for the carbons studied.

† Electronic supplementary information (ESI) available: experimental: preparation of the graphitized colloid-impregnated carbon. See http://www.rsc.org/suppdata/cc/b2/b200702a/

DOI: 10.1039/b200702a

mesopores. An interesting feature of the hysteresis loop of our samples is that both adsorption and desorption branches are quite vertical and parallel showing the presence of agglomerates of approximately uniform spherical mesopores as well as the narrow pore size distribution. This is consistent with the TEM observation of ungraphitized carbon.[14] To the best of our knowledge, this type of hysteresis has never been observed for graphitized carbons. The pore structure parameters evaluated from nitrogen adsorption are listed in Table 1. The specific surface area and the total pore volume decreased after graphitization. About half of the specific surface area and the pore volume is retained, which is substantially different from conventional activated carbons; their BET surface area typically decreases dramatically after graphitization, as illustrated in Table 2. Both small-angle X-ray scattering and the BET method show a surface area collapse for a microporous Saran char of $\sim 1200\ m^2\ g^{-1}$. Interestingly, the SAXS study of Chiche *et al.*[16] suggests that the admittedly broad pore size distribution of coal char-derived carbons is preserved after high temperature treatment. However, the porous structure revealed by SAXS may be closed and/or exhibit very narrow pore entrances, which are not accessible to N_2 at −196 °C and may also be inaccessible to other adsorbates at higher temperatures. In contrast, the high temperature treatment of the colloid-imprinted carbon did not reduce the accessibility of the porous structure but even caused its improvement, as evidenced by an increase in the pore size openings (see below).

Table 1 Adsorption parameters for the carbons studied

Sample[a]	BET surface area/$m^2\ g^{-1}$	Pore volume/$cm^3\ g^{-1}$	Pore diameter[b]/nm
CIC-24C	425	1.57	23.6
CIC-24C-G	239	0.72	16.5
Carbopack X	225	0.48	~7

[a] Carbopack X is a commercial graphitized carbon from Supelco, Inc. [b] Pore diameter at maximum of the pore size distribution.

Table 2 Effect of heat treatment on the surface area ($m^2\ g^{-1}$) of selected conventional high-surface-area carbons

	Coal char[16]		Saran char[a]	
Temp/°C	SAXS area[b]	BET area[c]	SAXS area[b]	BET area[c]
~2500	540	~0	4.3	0.4

[a] Saran char is produced by heat treatment of Saran (a product of Dow Chemical Co.) at *ca.* 1000 °C. [b] Surface area evaluated by small-angle X-ray scattering (SAXS). [c] Surface area evaluated from nitrogen adsorption by the BET method.

The adsorption hysteresis and pore size distributions (see inset in Fig. 1) show the presence of interconnected uniform spherical mesopores. It is noteworthy that the adsorption branch shifts to lower relative pressure while the desorption branch shifts slightly to higher relative pressure after graphitization. The shift of the adsorption branch is related to structural shrinkage during graphitization, which causes some reduction of the resulting pore size. Meanwhile, the desorption branch shift reflects some increase in the opening (interconnection) between spherical mesopores during graphitization. In addition, graphitization eliminates high-energy sites on the surface and increases surface homogeneity, which is manifested in Fig. 2 by remarkably low uptake at low relative pressures ($p/p_o < 10^{-4}$). It is also found that the surface area and the adsorption isotherm of the graphitized sample studied are similar to that measured on

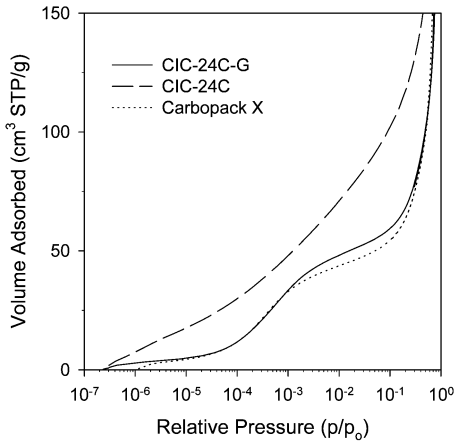

Fig. 2 Nitrogen adsorption isotherms for the carbons studied presented on a semi-logarithmic scale.

the graphitized carbon black Carbopack X from Supelco, Inc. Both nitrogen adsorption isotherms exhibit an apparent step reflecting monolayer formation ($p/p_o = 10^{-4}$–10^{-3}), which is characteristic for graphitized carbons.[17] Nevertheless, capillary condensation inside mesopores of Carbopack X takes place in a broad pressure range ($p/p_o = 0.75$–0.95) indicating a much wider pore size distribution.

In conclusion, this work shows that heat-treated ('graphitized') carbons with uniform spherical mesopores, narrow pore size distribution, high pore volume and high surface area can be synthesised *via* colloidal imprinting using a synthetic mesophase pitch as precursor. In contrast to conventional active carbons, the colloid-imprinted carbons survive the graphitization process, which is manifested by preserving the shape of mesopores and retaining the high surface area. In addition, the mechanical strength of such carbons is expected to be high because of the nature of the mesophase pitch precursor, which is used to produce high-performance carbon fibres. The simplicity, reproducibility and versatility of this synthetic approach make it amenable to commercial scale-up.

Notes and references

1 T. Kyotani, *Carbon*, 2000, **38**, 269.
2 S. Han, K. Sohn and T. Hyeon, *Chem. Mater.*, 2000, **12**, 3337.
3 H. Tamon, H. Ishizaka, T. Yamamoto and T. Suzuki, *Carbon*, 1999, **37**, 2049.
4 F. Bruner, G. Bertoni and P. Ciccioli, *J. Chromatogr.*, 1976, **120**, 307.
5 J. K. Knox and B. Kaur, *J. Chromatogr.*, 1986, **352**, 3.
6 J. Klett, R. Hardy, E. Romine, C. Walls and T. Burchell, *Carbon*, 2000, **38**, 953.
7 R. Ryoo, S. H. Joo and S. Jun, *J. Phys. Chem. B*, 1999, **103**, 7743.
8 M. Kruk, M. Jaroniec, R. Ryoo and S. H. Joo, *J. Phys. Chem. B*, 2000, **104**, 7960.
9 S. Jun, S. H. Joo, R. Ryoo, M. Kruk, M. Jaroniec, Z. Liu, T. Ohsuna and O. Terasaki, *J. Am. Chem. Soc.*, 2000, **122**, 10712.
10 A. A. Zakhidov, R. H. Baughman, Z. Iqbal, C. X. Cui, I. Khayrullin, S. O. Dantas, J. Martis and V. G. Ralchenko, *Science*, 1998, **282**, 897.
11 S. Han and T. Hyeon, *Chem. Commun.*, 1999, 1955; S. Han and T. Hyeon, *Carbon*, 1999, **37**, 1645.
12 G. Gundiah, A. Govindaraj and C. N. R. Rao, *Mater. Res. Bull.*, 2001, **36**, 1751.
13 J. S. Yu, S. B. Yoon and G. S. Chai, *Carbon*, 2001, **39**, 1421.
14 Z. J. Li and M. Jaroniec, *J. Am. Chem. Soc.*, 2001, **123**, 9208.
15 J. Rouquerol, D. Avnir, C. W. Fairbridge, D. H. Everett, J. H. Hayness, N. Pernicone, J. D. F. Ramsay, K. S. W. Sing and K. K. Unger, *Pure Appl. Chem.*, 1994, **66**, 1739.
16 P. Chiche, S. Durif and S. Pregermain, *Fuel*, 1965, **44**, 5.
17 M. Kruk, Z. J. Li and M. Jaroniec, *Langmuir*, 1999, **15**, 1435.